ACS APPLIED MATERIALS & INTERFACES

www.acsami.org

Forum Article

3D-Printed Multi-Stimuli-Responsive Mobile Micromachines

Yun-Woo Lee,[†] Hakan Ceylan,[†] Immihan Ceren Yasa, Ugur Kilic, and Metin Sitti*

Cite This: *ACS Appl. Mater. Interfaces* 2021, 13, 12759–12766

Read Online

ACCESS | Metrics & More | Article Recommendations | Supporting Information

ABSTRACT: Magnetically actuated and controlled mobile micromachines have the potential to be a key enabler for various wireless lab-on-a-chip manipulations and minimally invasive targeted therapies. However, their embodied, or physical, task execution capabilities that rely on magnetic programming and control alone can curtail their projected performance and functional diversity. Integration of stimuli-responsive materials with mobile magnetic micromachines can enhance their design toolbox, enabling independently controlled new functional capabilities to be defined. To this end, here, we show three-dimensional (3D) printed size-controllable hydrogel magnetic microscrews and microrollers that respond to changes in magnetic fields, temperature, pH, and divalent cations. We show two-way size-controllable microscrews that can reversibly swell and shrink with temperature, pH, and divalent cations for multiple cycles. We present the spatial adaptation of these microrollers for penetration through narrow channels and their potential for controlled occlusion of small capillaries (30 μm diameter). We further demonstrate one-way size-controllable microscrews that can swell with temperature up to 65% of their initial length. These hydrogel microscrews, once swollen, however, can only be degraded enzymatically for removal. Our results can inspire future applications of 3D- and 4D-printed multifunctional mobile microrobots for precisely targeted obstructive interventions (e.g., embolization) and lab- and organ-on-a-chip manipulations.

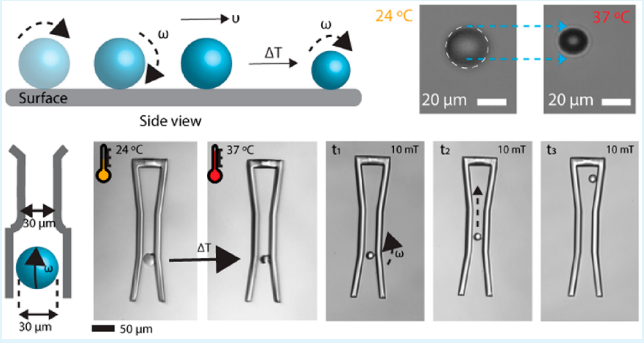

KEYWORDS: *stimuli-responsive materials, micromachine, 3D printing, 4D printing, microrobot*

INTRODUCTION

Magnetic mobile micromachines have become promising tools that could empower wireless lab-on-a-chip manipulations and minimally invasive targeted therapies by providing spatially precise and temporally on-demand manipulation control in small and hard-to-access spaces.[1−4] To realize such potential, various mobile magnetic micromachines have been proposed for different biomedical applications, such as targeted cargo delivery,[5,6] cell manipulation,[7−9] and tissue engineering.[10] Despite the sheer progress in the magnetic actuation, locomotion, and control capabilities,[11−13] a majority of the reported micromachines so far have been made from passive backbone materials,[14] which limits their functional capabilities. To overcome this limitation and increase the capabilities of the magnetic micromachines to execute multiple tasks that are controlled from independent inputs, integration of stimuli-responsive materials can be a key enabler.

Four-dimensional (4D) printing has recently unleashed a potential for the programming of stimuli-responsive materials that exhibit various size-controlling and shape-morphing behaviors.[15] 4D-printed materials can morph their shape through one-way (irreversible) or two-way (reversible) body deformations under mild and biologically favorable environmental conditions.[16] The mechanism underlying these material deformations entails controlled expansion and contraction of three-dimensional (3D)-printed structures in response to a wide variety of external chemical or physical stimuli, such as magnetic fields,[17] temperature,[18,19] pH,[20] and light.[21]

Motivated by the integration of magnetic micromachines with size-controllable soft materials at the smaller length scales, researchers demonstrated two magnetic milli-swimmer designs by using a thermoresponsive two-way size-controllable polymer in the backbone.[22,23] The swimmer could adapt its swimming properties to the changes in the environmental temperature. Another very recent untethered magnetic microgripper has exhibited a one-way thermoresponsive size-controllable behavior for a potential single-cell-size biopsy application.[24] Apart from these 2D-to-3D folding material fabrication approaches, to the best of our knowledge, there has been so far no report on the use of 3D-printed untethered multifunctional micromachines made from size-controllable polymers that would enable the execution of new functional capabilities in addition to and independent from its magnetic steering and propulsion control.

Special Issue: Novel Stimuli-Responsive Materials for 3D Printing

Received: October 10, 2020
Accepted: December 18, 2020
Published: December 30, 2020

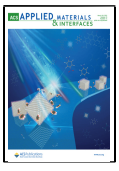

Here, we design and 3D print untethered microscrews and microrollers that exhibit one-way and two-way size-controllable behaviors by responding to four different stimuli: magnetic fields, temperature, pH, and calcium ions. We show alternative size-control strategies that may inspire more customized future designs. For example, we show that two-way size-controllable microscrews can reversibly swell and shrink with temperature, pH, and divalent cations for multiple cycles. It is a powerful approach to decouple the control inputs of magnetic propulsion/steering and shape change behaviors, while introducing redundancy in the shape change control by temperature, pH, and divalent cations in logically controlled patterns can enhance the adaptability of the functional task to various unstructured environments. We further show one-way size-controllable microscrews that can swell with temperature up to 65% of its initial length. These microscrews, however, can only be degraded enzymatically for removal, once swollen. Finally, we present a proof-of-the-concept potential of two-way size-controllable microrollers for penetration through narrow channels and their potential for controlled occlusion of small capillaries with 30 μm diameter. Our results can inspire future applications of 3D- and 4D-printed multifunctional microrobots for precisely targeted obstructive interventions and lab/organ-on-a-chip manipulations.

RESULTS

We selected microroller[25] and helical microscrew[26] models as two representative designs for the proof-of-concept demonstration of the multi stimuli-responsive magnetic micromachines. We 3D-printed these designs from one-way and two-way shape memory polymers that respond differently to external stimuli (Figure 1a).

For two-way shape memory effect, we formulated a magnetic and thermoresponsive precursor mixture by utilizing poly *N*-isopropylacrylamide (pNIPAM) as shown on Figure 1b. Hydrogels of pNIPAM typically exhibit low critical solution temperature (LCST) behavior.[34] Below its LCST, the polymer chains of pNIPAM are hydrophilic and form hydrogen bonds with water molecules when immersed in aqueous solution. Hence, the hydrogel network of pNIPAM expands with the water absorption below its LCST. As temperature increases above the LCST, the polymer chains of pNIPAM undergoes a transition that result in expulsion of water out of its network and shrinkage. To date, microactuators with complex 3D geometries and from various polymeric materials, such as *N*-isopropylacrylamide, acrylic acid, β-cyclodextrin acrylamide (βCD-AAm), and adamantane acrylamide (Ad-AAm), have been reported.[20,31−33]

In addition to thermoresponsiveness, we introduced pH and ion responsiveness by formulating the precursor mixture *N*-isopropylacrylamide with acrylic acid (pNIPAM-AAc) in the form of a copolymer. Carboxylic acid groups on the acrylic acid can respond to pH and the presence of divalent ions due to the transition in its protonated/deprotonated states and charge screening, respectively. Upon exposure to an aqueous solution with a pH value above its acidity constant (pK_a), the −COOH group on the polymer chains deprotonates and creates the negatively charged $-COO^-$ group. The negatively charged molecular chains absorb more water, driving a significant expansion of the network size. Reversely, the carboxylate groups will be protonated when the pH value is lower than its pK_a, driving off the water molecules and hence shrunk network size. We also sought to control the swelling properties with charge

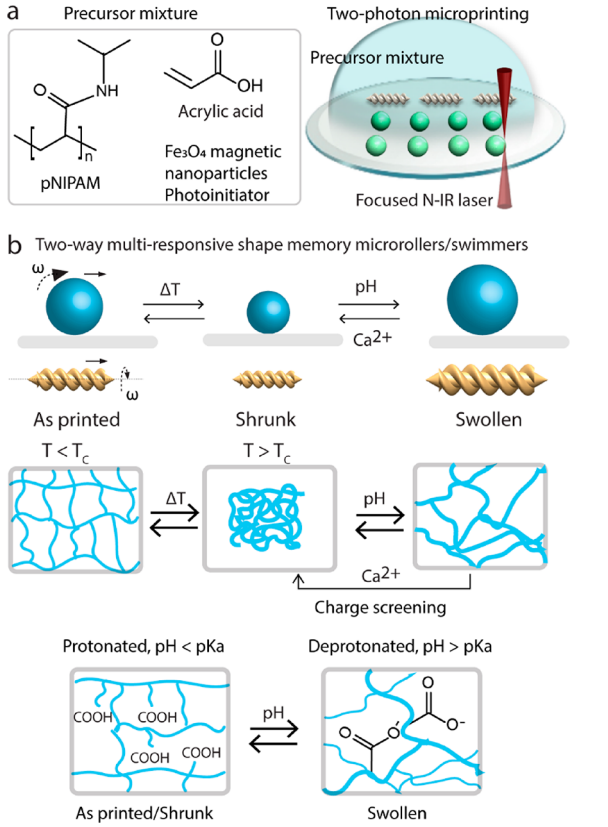

Figure 1. Schematic illustration of 4D printing of size-controllable microrollers and microscrews using external stimuli. (a) Schematic illustration of the components of stimuli-responsive material-based photoresists and printing process using a direct laser writing (two-photon polymerization) system. (b) Schematic representation of the two-way size-controllable microrollers/microscrews mechanism when induced by multiple stimuli, such as temperature, pH, and Ca^{2+} ions.

screening, depending on the presence or absence of Ca^{2+} ions in solution. When the hydrogel is exposed to divalent Ca^{2+} ions, the carboxylate groups are screened via by means of Ca^{2+} ions. On the contrary, removing Ca^{2+} ions within the network leads to swelling of the micromachines.

To realize such 3D geometries with a stimuli-responsive material, we fabricated microrollers and microscrews using two-photon polymerization-based 3D printing. Briefly, the interaction of the focused femtosecond laser (wavelength of 780 nm) irradiation with the photoinitiator in a tight focal volume, called voxel, results in the initiation of a free-radical polymerization with the electrons of π bonds within the precursor monomers. Computer-controlled scanning of the laser within the bulk volume of the precursor mixture solution thus facilitates the formation of complex 3D microstructures with submicrometer (as low as 100 nm) features.[27−30]

To realize a fully reversible two-way response with the microrollers and microscrews, we prepared a photocurable resin containing pNIPAM-AAc. We first optimized the fabrication process by applying different laser doses for the maximized structural fidelity of microscrews in three different dimensions (Figure S1). Figure 2a demonstrates the 3D-printed illustrations of microrollers with different laser powers. Between 15 and 35 mW with a 20×10^3 μm s^{-1} scanning speed, the microroller shows acceptable dose and the structural fidelity of the printed microrollers was in agreement with the design.

https://dx.doi.org/10.1021/acsami.0c18221
ACS Appl. Mater. Interfaces 2021, 13, 12759−12766

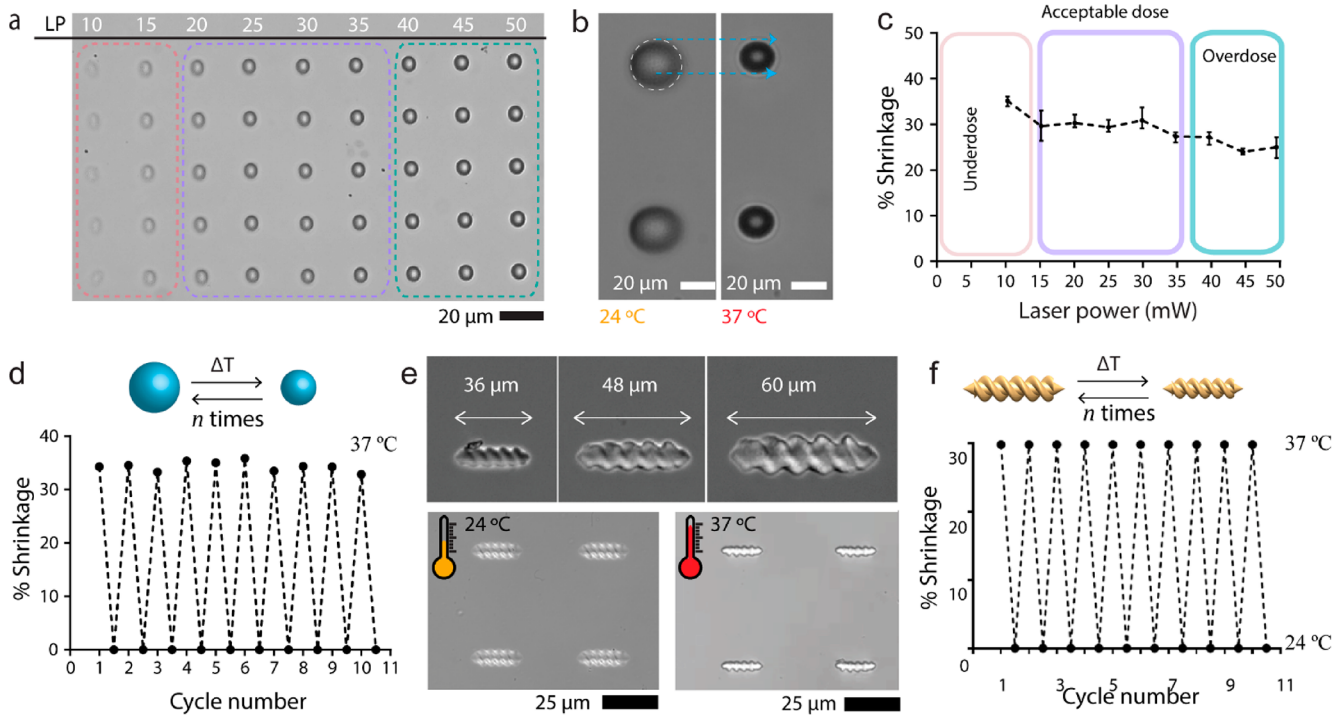

Figure 2. Temperature responsiveness of two-way size-controllable spherical microrollers and double-helical microscrews. (a) Optical microscopy images of the 3D-printed pNIPAM-AAc microrollers (the unit of laser power (LP) is mW). (b) Optical microscopy images of shrinkage of the microrollers in response to change in temperature. (c) Plot showing the relationship between the laser power for printing the material and resulting shrinkage properties due to the change in the cross-linking density. Different laser powers ranging from 0 to 50 mW were exposed to microrollers composed of pNIPAM-AAc. (d) The repetition test of the pNIPAM-AAc microrollers shrinking/deshrinking cycles without any deterioration. (e) Optical microscopy images of three different microscrews printed in different sizes and representative swelling/deswelling of a 4 × 4 microscrews array in response to temperature change. (f) Repetition test of the pNIPAM-AAc microscrews during temperature-dependent shrinking/deshrinking cycles.

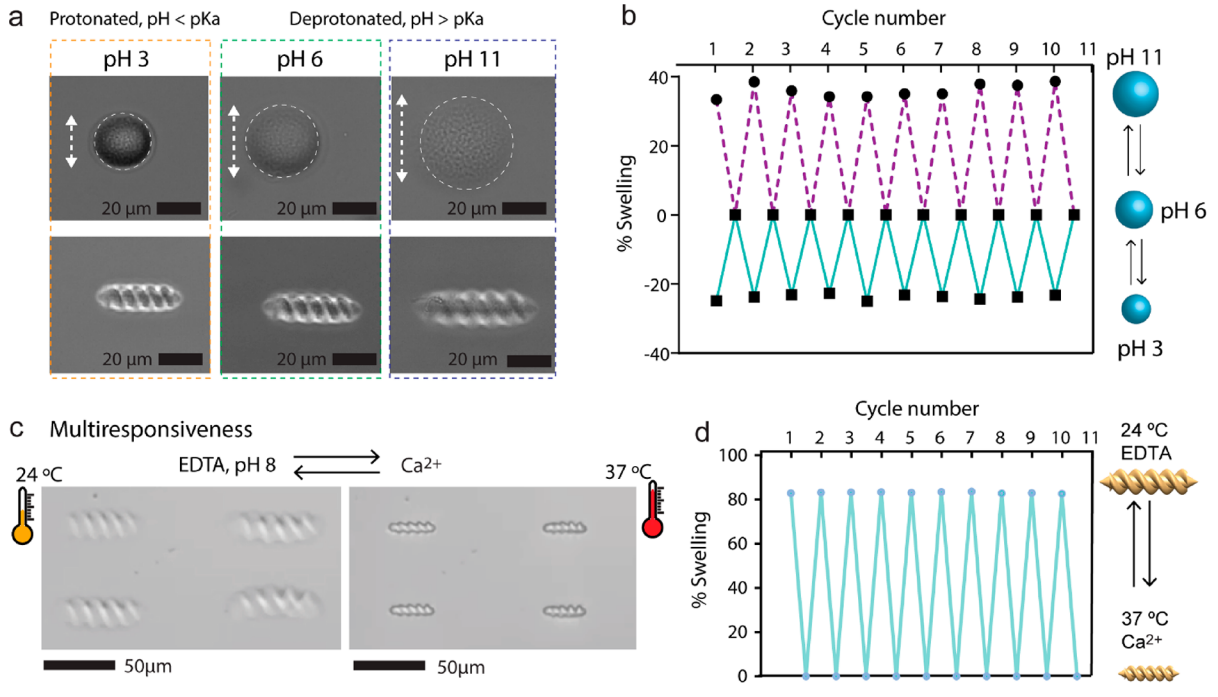

Figure 3. pH and ion responsiveness of two-way size-controllable microrollers and microscrews. (a) Optical images of swelling/deswelling microrollers and microscrews in response to pH value. (b) The repetition test of the pNIPAM-AAc microrollers swelling cycles in response to pH. (c) Optical images of multiresponsiveness of microscrews in response to temperature and Ca^{2+} ion concentration change. (d) Repetition test of the pNIPAM-AAc microscrews shrinking/swelling cycles in response to temperature and Ca^{2+} ion change.

To investigate the reversible swelling and shrinking characteristics of the pNIPAM-AAc-based spherical microrollers, fabricated microrollers were immersed in water at room temperature and the temperature was then elevated to 37 °C

https://dx.doi.org/10.1021/acsami.0c18221
ACS Appl. Mater. Interfaces 2021, 13, 12759−12766

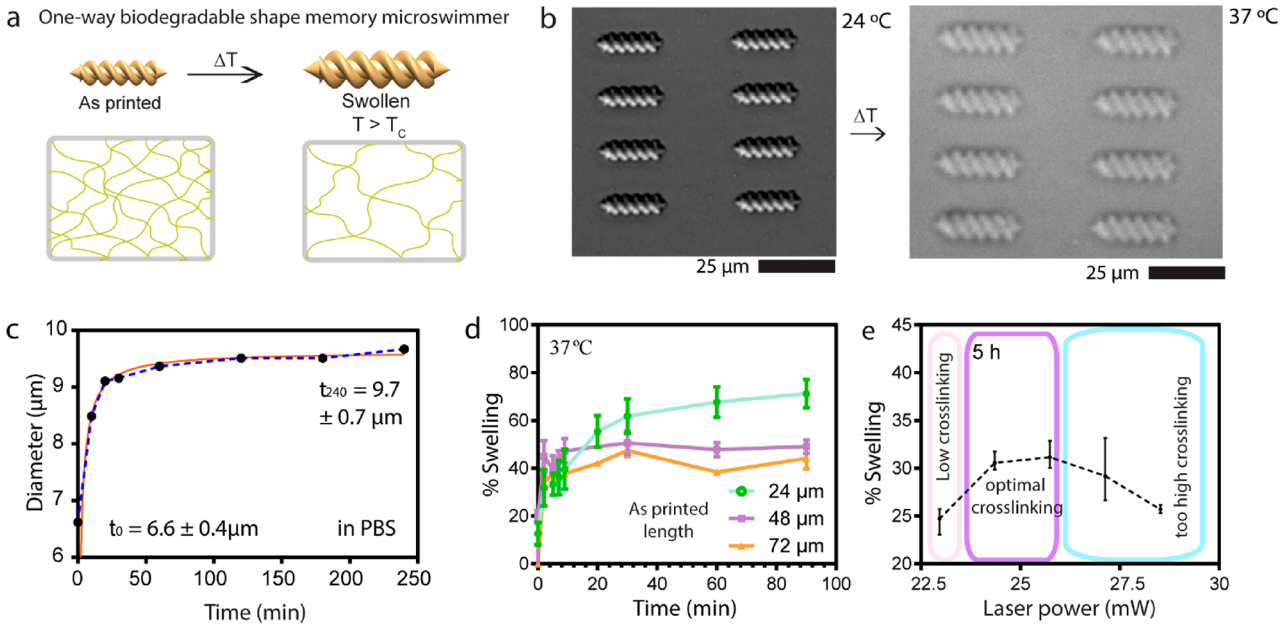

Figure 4. Temperature responsiveness of one-way size-controllable double-helical microscrews. (a) Schematic representation of one-way size-control mechanism by temperature change. (b) Optical microscopy images of gelatin-based microscrews swelling in response to temperature change. (c) Swelling kinetics of gelatin-based microscrews in PBS. (d) Swelling kinetics of different sizes of gelatin microscrews in response to temperature. (e) Effect of the laser power on the cross-linking and swelling of gelatin-based microscrews.

as shown in Figure 2b. When the temperature is only slightly over the LCST of pNIPAM (around 32 °C), the hydrogel microrollers exhibited deswelling behavior due to the hydrophilic-to-hydrophobic phase change. The body length of the microrollers changed to 34% of their original length when they were exposed to the temperature change. Upon the microrollers being cooled back to the room temperature, the structures became hydrophilic again and were restored to their initial state by swelling with water. In addition, to investigate the effect of the cross-linking density on the temperature-responsive behavior of pNIPAM microrollers, we utilized different laser parameters during the printing process of the microrollers and observed the change in their swelling characteristics. We defined a swelling rate of microrollers as the ratio of the length change to the initial length as

$$\varepsilon(\%) = -\frac{l_0 - l}{l_0}100$$

where l and l_0 are the length of the expanded and original microrollers, respectively. Figure 2c demonstrates how the printing laser parameters change the swelling property of the microrollers in response to temperature. As laser power increases from 10 to 50 mW, the shrinkage rate decreases by 20%. This result indicates the effect of the cross-linking density of the printed microrollers on their swelling kinetics. Slower scanning speed and higher laser power provided the higher cross-linking density of the material, which limits the swelling performance of the pNIPAM-AAC microrollers. (Figure S2). The swelling and shrinkage of microrollers were performed multiple times by sequential heating and cooling cycles without observing any plastic deformation on the structures (Figure 2d).

In addition to microrollers, we demonstrated the printing of our previous double-helical geometry,[6] which is more complex in shape compared to microrollers. Such a microscrew design aims to maximize the volume of the body for potential high-volume cargo delivery applications. Figure 2e demonstrates that we were able to print different size (36, 48, and 60 μm body length) of helical microscrews from stimuli-responsive material formulation. The structural fidelity of the resulting microscrews was in agreement with the proposed computer-aided design. To study the temperature responsiveness of the resulting pNIPAM-based microscrews, we raised the temperature to 37 °C, which is above the phase volume transition, and the fabricated microscrews exhibited length shrinkage by 30% (Figure 2e). At low temperatures, they showed swelling back to their initial length. We also investigated the robustness of the structures and reversibility of the length change by performing multiple cycles of heating and cooling (Figure 2f). Similar to the spherical microrollers, we were able to demonstrate multiple cycles of swelling and deswelling without any noticeable damage in the double-helical microscrews shape.

Concerning the pH-responsive characteristics of the pNIPAM-AAc hydrogels, microrollers, and microscrews were printed and initially placed in water (Figure 3a). Because a large number of carboxy groups in the polymer chain, we expect to observe the deprotonation of carboxylic acid groups and electrostatic repulsion between the ionized chains which leads to a significant expansion of the network by absorbing water upon treatment with high pH solutions. Therefore, the addition of ammonia solution with a pH value of 11 led to the expansion of the microrollers and microscrews up to 40% in body length. The response of the microstructures was within seconds because of the fast diffusion rate of ions. On the contrary, by dropping inside a low pH solution, the microroller and microscrews lengths shrunk rapidly by 22% with the protonation of carboxylic acid groups. The swelling and shrinking process were fully reversible and can be repeated many times as shown in Figure 3b.

We also investigated the ion-responsive properties of the pNIPAM-AAc hydrogels (Figure S3). Upon adding a chemical such as ethylenediaminetetraacetic acid (EDTA) into the hydrogels in water, their size became expanded because it

https://dx.doi.org/10.1021/acsami.0c18221
ACS Appl. Mater. Interfaces 2021, 13, 12759−12766

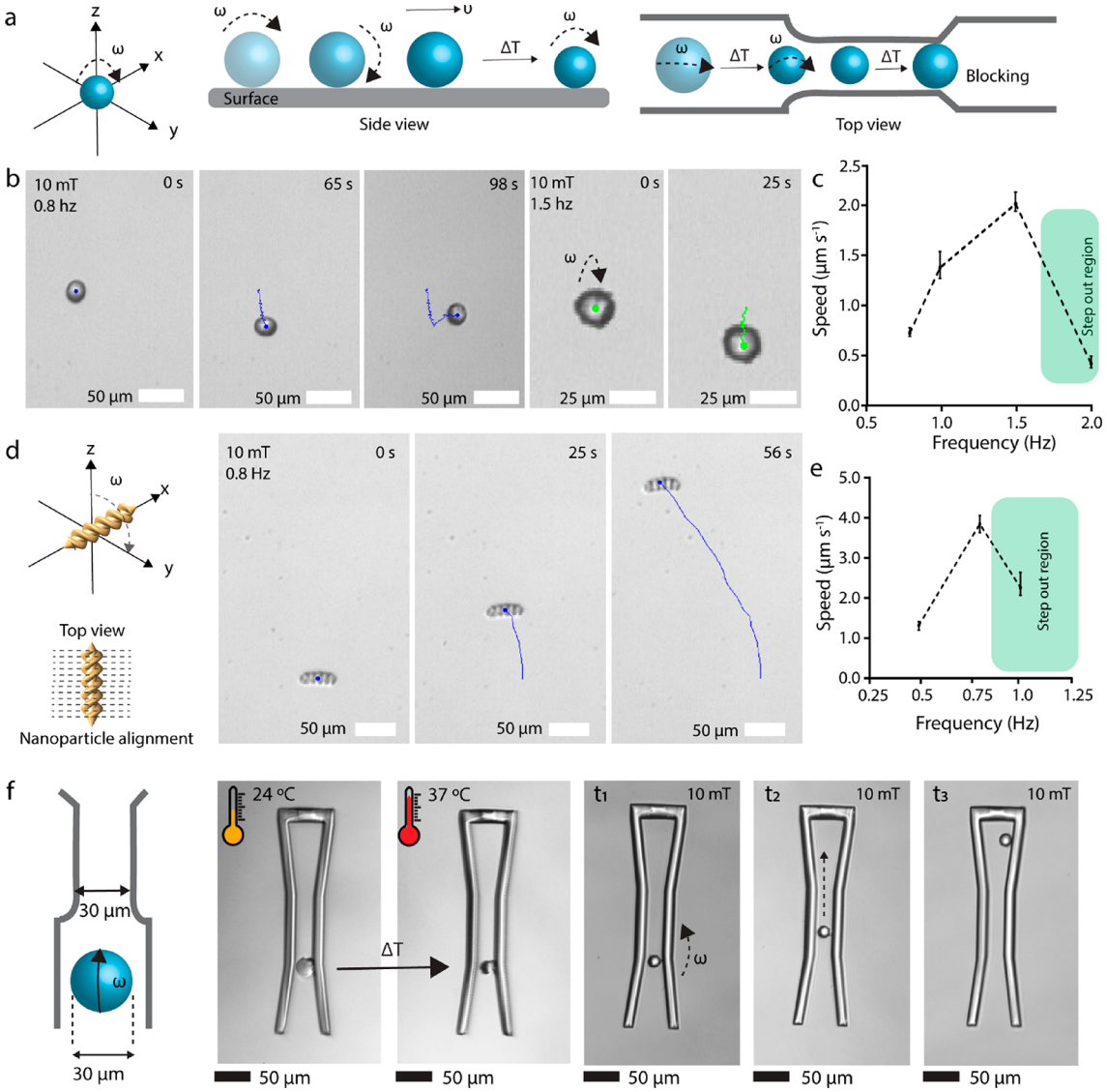

Figure 5. Actuation and steering demonstrations of the microrollers and microscrews using a rotating magnetic field, and demonstration of their spatial adaptability by their temperature-dependent size control. (a) Schematic illustration of magnetic actuation and steering of the microrollers. (b) Controlled surface rolling trajectory snapshots (blue lines) of a microroller at a 10 mT rotating magnetic field at 0.8 and 1.5 Hz on a smooth glass substrate inside deionized water. (c) Mean motion speed of the microrollers as a function of magnetic rotation frequency. (d) Magnetic steering control snapshots of the double-helical microscrews at 10 mT rotating magnetic field at 0.8 Hz. (e) Mean speed of microscrews with different rotation frequencies. (f) Schematic diagram and optical images of the microroller showing the spatial adaptability (shrinkage) by temperature control to pass through a channel smaller than its initial diameter.

contains carboxyl groups in the hydrogel. The carboxylic groups in acrylic acid (AAc) can release protons and thus be ionized. The repulsive forces of carboxylate ions repel other molecular chains to expand the size of the hydrogel. When exposed to Ca^{2+} solutions, the carboxyl groups accept protons and thus be deionized and shrunk their structure. The swelling and shrinking process were fully reversible and can be repeated for multiple cycles. By dropping a sufficient amount of EDTA solution, the structures could swell up quickly to 140% of its size, and the whole process completed in a few seconds. When $CaCl_2$ solution was injected, the original state is recovered within seconds. To achieve a high swelling/deswelling ratio, we adopted multi-responsiveness to temperature and Ca^{2+} ions as shown in Figure 3c. By exploiting this synergistic property, a single hydrogel can be actuated to have the capability of a responsive direction, which they can shrink in response to heat and swell in response to Ca^{2+} ions. The body length of the microscrews was changed 36% of their original length in response to temperature and they became swollen up to 80% of their length compared to the shrunk state of the microscrews. In addition, to confirm the reversibility of the actuation process, we conducted the same process 10 times and there was no deterioration as shown in Figure 3d.

We previously introduced gelatin-based magnetic nanocomposites as two-photon-based 3D printable and biodegradable materials.[6] To further study one-way size-controllable polymer, we utilized this material because of its inherent temperature-responsive behavior as shown on Figure 4a. Gelatin derived from the hydrolysis of collagen is a temperature-sensitive material. Its cross-linked form exhibits swelling behavior in response to an increase in temperature and its network is enzymatically degradable.[6,35] To investigate the one-

https://dx.doi.org/10.1021/acsami.0c18221
ACS Appl. Mater. Interfaces 2021, 13, 12759−12766

way size-controllable behavior of gelatin-based microscrews, we microscopically monitored the shape transformation by increasing the room temperature, where microscrews were in their printed size, to 37 °C. We observed the swelling of the microscrews body by 23.4% upon increasing temperature to 37 °C (Figure 4b). Also, the diameter of 24 μm length microscrews increased to 9.7 ± 0.7 μm from 6.6 ± 0.4 μm in 4 h (Figure 4c). To study the size-dependence of gelatin-based microscrews swelling, we 3D printed the microscrews in different dimensions (24, 48, and 72 μm length) and increased the temperature to 37 °C. From the study, we observed that increasing the dimensions of the microscrews resulted in decreased overall swelling degree as shown in Figure 4d. Further, we investigated the impact of the laser power on the swelling property of the one-way size-controllable microscrews in response to temperature as shown in Figure 4e. As the laser power increased from 22.5 to 25 mW, the swelling rate followed a sharp increase due to the formation of new network chains to absorb additional water. After reaching the optimal cross-linking density at 25 mW, over-cross-linking resulted in another sharp drop in the swelling. High degree of cross-linking led to decrease in the pore size of the gelatin, so that water molecules are expelled.

As shown in Figure 5a, we present the magnetically steerable 3D-printed microroller. For the mobility of the micromachines, we encapsulated superparamagnetic iron oxide nanoparticles (SPIONs) inside the pNIPAM-AAc. The total amount of SPIONs loaded in the mesh network of the micromachine body is crucial for their swelling ratio. Increasing the amount would result in a lower shrinking ratio. Increased volume fraction of the SPIONs from 0 to 0.33 shrunk from 36% to 27% (Figure S4). Over 0.33 of the volume fraction, 3D printing was not possible, likely due to the reduced degree of percolation of the cross-linked network.[36] Introduction of SPIONs could induce steric hindrances inside the pNIPAM polymer network, which changes their swelling kinetics. For magnetic mobilization, we utilized a custom five-coil electromagnetic setup to create rotating uniform magnetic fields that rotate/propel and steer microrollers and microscrews along designated trajectories (Figures 5b, d). We characterized the frequency-dependent behavior of the microrollers and microscrews loaded with 4.2 mg mL^{-1} SPIONs at 10 mT. As increasing the input frequency starting from 0.5 to 2 Hz, the speed of the microroller increased up to 1.96 μm s^{-1} and optimally controlled microrollers at 1.5 Hz (Figure 5c). Additionally, we characterized the speed of the microroller in response to temperature. As shown in Figure S5, it decreased as the temperature was increased to 37 °C. We also investigated the step-out frequency of the microscrews by gradually increasing the frequency of the applied rotating magnetic field from 0.5 to 1 Hz. It was demonstrated that the fabricated microrollers were actuated and steered optimally at 0.8 Hz under a 10 mT rotating magnetic field (Figure 5e). The velocity of the microscrews at optimum actuation frequency was measured to be 2.7 μm s^{-1}.

To further test the spatial adaptability and motion capability of stimuli-responsive microrollers, we prepared a microfluidic channel with the same body length of initial microrollers (30 μm channel diameter), so that the microrollers could not pass through the channel unless they changed their size. We steered the microrollers to the beginning of the channel and changed the temperature to induce temperature-dependent shrinkage. After microrollers shrunk to the size smaller than 30 μm, they could pass through the channel. Then, we actuated the microrollers with a frequency of 2 Hz to steer them within the channels in a controlled manner (Figure 5f and Video S3). Such capability can inspire to use this method for controlled chemoembolization of tumor tissues at distal arteries and arterioles. Currently, embolization methods are available only for large arteries by using passive particles. This limits the potential of clinically used embolization methods to target tumors precisely and these methods can also damage the healthy organ sites. Our method has the potential to leverage the capability of the chemo-embolization by specifically reaching out to smaller vessels in a steerable way. The swollen-state microrollers can be moved through the channels, and as the channel size narrows down, the externally heated and shrinking microrollers can go further down until it efficiently clogs the vessel at a distal location. The shrinkage can also be accompanied by the release of chemo-therapeutics that can be sequestered within the hydrogel body of the microrollers. Both one-way and two-way micromachines are alternative design strategies that can provide unique advantages depending on the context. Two-way shape-memory micro-machines can reversibly go through smaller channels. However, they are not biodegradable; therefore, in cases where shrinking the size might be needed without an environmental stimuli, it might be difficult to retrieve them. One-way shape memory-based irreversible micromachines can swell and clog the channels that are bigger than their size. These micromachines are biodegradable, which is a significant property for future in vivo applications. Although two-way reversible micromachines can go through smaller channels, one-way irreversible micro-machines can clog the channels that are bigger than their size.

CONCLUSION

We present the combination of magnetically steerable 3D-printed microroller and microscrews designs with stimuli-responsive hydrogel materials to develop size-controllable micromachines. These wirelessly controlled micromachines gained the ability to respond to multiple stimuli, including magnetic fields, temperature, pH, and cations. We show the multiresponsive behavior as a powerful approach to decouple the control inputs of magnetic propulsion/steering and shape change behaviors and to introduce redundancy in the shape change control by temperature, pH, and divalent cations in logically controlled patterns, which can enhance the adaptability of the micromachines to various unstructured environments. Although two-way reversible micromachines can go through smaller channels, one-way irreversible micromachines can clog the channels that are bigger than their size. Additionally, one-way micromachines are biodegradable, which makes them more suitable for future in vivo medical applications. Our results can inspire future applications of 3D- and 4D-printed multifunctional microrobots for precisely targeted obstructive interventions and lab/organ-on-a-chip manipulations.

MATERIALS AND METHODS

Materials. *N*-Isopropylacrylamide (NIPAM, Scientific Polymer Products Inc.), poly(*N*-isopropylacrylamide) (PNIPAM, Scientific Polymer Products Inc.), *N*,*N*′-methylenebis-acrylamide (BIS, Sigama-Aldrich), acrylic acid (AAc, Sigma-Aldrich), lithium phenyl-2,4,6-trimethylben zoylphosphinate (LAP, Tokyo Chemical Industry Co. Ltd.), iron oxide nanoparticles coated with poly(ethylene glycol) amine of 50 nm hydrodynamic size (Chemicell GmbH, Germany).

Synthesis of pNIPAM-AAc Solution. To prepare precursor pNIPAM-AAc solution, 3000 mg of NIPAM monomer, 400 mg of pNIPAM, and 180 mg of BIS were dissolved overnight in 10 mL of ethylene glycol under constant stirring (600 rpm) at room temperature. To this solution, 300 μL of solution AAc (w/w) was added followed by

https://dx.doi.org/10.1021/acsami.0c18221
ACS Appl. Mater. Interfaces 2021, 13, 12759−12766

3.5% (w/w) photoinitiator addition. The resultant mixture was stirred again (600 rpm) at room temperature until all the components were dissolved. Iron oxide nanoparticles (4.2 mg mL^{-1}) and the resultant precursor solution were then mixed by vortex mixing and ultrasound sonication. The resulting precursors was preserved in yellow light conditions to avoid unnecessary exposure.

Fabrication of the Microrollers and Microscrews. The prepolymer mixture was dropped on a trichloro(1H,1H,2H,2H-perfluorooctyl)silane-treated glass slide. Printing was performed with a commercial direct laser writing setup (Photonic Professional GT, Nanoscribe GmbH) with a 25×, NA = 0.8 oil immersion objective. Polymerization of the solution in predefines structures was performed in a closed channel, which had two sites to place permanent magnets for the alignment of magnetic particles. After the fabrication, the sample is immersed in isopropyl alcohol for 30 min to remove the uncured precursor. The developed microscrews were placed in water.

Characterization. To analyze the response of the samples to changes in temperature, pH, and ion concentration we acquired time-lapse images using a Nikon Eclipse Ti-E microscope at 10× and 20× magnification in the DIC mode. We used 2-(N-morpholino)-ethanesulfonic acid (MES) buffer at pH value of 3 and 6 for the pH response experiments.

Magnetic Actuation and Control of the Microscrews and Microrollers. Both microscrews and microrollers were actuated and steered using a five-coiled electromagnetic setup, which can be mounted on an inverted optical Zeiss microscope. (Zeiss Axio Observer A1) The experiments were performed under a 10 mT rotating magnetic field. The step-out frequencies were determined by gradually increasing the frequency of rotating magnetic field from 0.5 to 2 Hz. For the mobility characterizations, an in-house particle tracking software developed in *MATLAB* (MathWorks, Natick, MA) was used.

■ ASSOCIATED CONTENT

Supporting Information

The Supporting Information is available free of charge at https://pubs.acs.org/doi/10.1021/acsami.0c18221.

Further optimization of the femtosecond laser fabrication process for the maximized structural fidelity of microscrews, influence of the fabrication parameters (laser power and scanning speed) and magnetic nanoparticle concentrations on actuation strain, and further two-way shape memory micromachine characterizations in response to systematic stimuli changes(PDF)

Video S1, stimuli-responsiveness of microrollers and microscrews (MP4)

Video S2, magnetic actuation and steering of microscrews and microrollers (MP4)

Video S3, spatial adaptability and motion of the stimuli-reponsive microrollers (MP4)

■ AUTHOR INFORMATION

Corresponding Author

Metin Sitti − *Physical Intelligence Department, Max Planck Institute for Intelligent Systems, Stuttgart 70569, Germany; School of Medicine and College of Engineering, Koc University, Istanbul 34450, Turkey; Institute for Biomedical Engineering, ETH Zurich, Zurich 8092, Switzerland;* orcid.org/0000-0001-8249-3854; Email: sitti@is.mpg.de

Authors

Yun-Woo Lee − *Physical Intelligence Department, Max Planck Institute for Intelligent Systems, Stuttgart 70569, Germany*

Hakan Ceylan − *Physical Intelligence Department, Max Planck Institute for Intelligent Systems, Stuttgart 70569, Germany*

Immihan Ceren Yasa − *Physical Intelligence Department, Max Planck Institute for Intelligent Systems, Stuttgart 70569, Germany;* orcid.org/0000-0002-5013-7246

Ugur Kilic − *Physical Intelligence Department, Max Planck Institute for Intelligent Systems, Stuttgart 70569, Germany; School of Medicine, Koc University, Istanbul 34450, Turkey*

Complete contact information is available at: https://pubs.acs.org/10.1021/acsami.0c18221

Author Contributions

†Y.L. and H.C. contributed equally to this work and should be considered co-first authors. Y.-L., H.C., and M.S. conceived and designed the study. Y.L. and U.K. performed the fabrication of the microscrews and the characterization of the stimuli responsiveness. Y.L. and I.C.Y. designed and performed the motility experiments. Y.L., H.C., I.C.Y., and U.K. analyzed the data. M.S. supervised the research and discussed the results. All authors contributed to the writing of the manuscript and gave their consent to the final version.

Notes

The authors declare no competing financial interest.

■ ACKNOWLEDGMENTS

The authors acknowledge funding from the Max Planck Society and European Research Council (ERC) Advanced Grant SoMMoR project with grant no: 834531.

■ REFERENCES

(1) Nelson, B. J.; Kaliakatsos, I. K.; Abbott, J. J. Microrobots for minimally invasive medicine. *Annu. Rev. Biomed. Eng.* **2010**, *12* (1), 55−85.

(2) Sitti, M.; Ceylan, H.; Hu, W.; Giltinan, J.; Turan, M.; Yim, S.; Diller, E. Biomedical Applications of Untethered Mobile Milli/Microrobots. *Proc. IEEE* **2015**, *103* (2), 205−224.

(3) Ceylan, H.; Giltinan, J.; Kozielski, K.; Sitti, M. Mobile microrobots for bioengineering applications. *Lab Chip* **2017**, *17* (10), 1705−1724.

(4) Li, J.; Esteban-Fernandez de Avila, B.; Gao, W.; Zhang, L.; Wang, J. Micro/Nanorobots for Biomedicine: Delivery, Surgery, Sensing, and Detoxification. *Sci. Robot* **2017**, *2* (4), eaam6431.

(5) Qiu, F. M.; Fujita, S.; Mhanna, R.; Zhang, L.; Simona, B. R.; Nelson, B. J. Magnetic Helical Microswimmers Functionalized with Lipoplexes for Targeted Gene Delivery. *Adv. Funct. Mater.* **2015**, *25* (11), 1666−1671.

(6) Ceylan, H.; Yasa, I. C.; Yasa, O.; Tabak, A. F.; Giltinan, J.; Sitti, M. 3D-Printed Biodegradable Microswimmer for Theranostic Cargo Delivery and Release. *ACS Nano* **2019**, *13* (3), 3353−3362.

(7) Yasa, I. C.; Tabak, A. F.; Yasa, O.; Ceylan, H.; Sitti, M. 3D-Printed Microrobotic Transporters with Recapitulated Stem Cell Niche for Programmable and Active Cell Delivery. *Adv. Funct. Mater.* **2019**, *29* (17), 1808992.

(8) Dong, M.; Wang, X. P.; Chen, X. Z.; Mushtaq, F.; Deng, S. Y.; Zhu, C. H.; Torlakcik, H.; Terzopoulou, A.; Qin, X. H.; Xiao, X. Z.; Puigmarti-Luis, J.; Choi, H.; Pego, A. P.; Shen, Q. D.; Nelson, B. J.; Pane, S. 3D-Printed Soft Magnetoelectric Microswimmers for Delivery and Differentiation of Neuron-Like Cells. *Adv. Funct. Mater.* **2020**, *30* (17), 1910323.

(9) Yasa, I. C.; Ceylan, H.; Bozuyuk, U.; Wild, A. M.; Sitti, M. Elucidating the interaction dynamics between microswimmer body and immune system for medical microrobots. *Sci. Robot* **2020**, *5* (43), eaaz3867.

(10) Tasoglu, S.; Diller, E.; Guven, S.; Sitti, M.; Demirci, U. Untethered micro-robotic coding of three-dimensional material composition. *Nat. Commun.* **2014**, *5* (1), 3124.

(11) Jiang, S.; Hu, Y.; Wu, H.; Zhang, Y.; Zhang, Y.; Wang, Y.; Zhang, Y.; Zhu, W.; Li, J.; Wu, D.; Chu, J. Multifunctional Janus Microplates

Arrays Actuated by Magnetic Fields for Water/Light Switches and Bio-Inspired Assimilatory Coloration. *Adv. Mater.* **2019**, *31* (15), e1807507.
(12) Zhu, S.; Bian, Y.; Wu, T.; Chen, C.; Jiao, Y.; Jiang, Z.; Huang, Z.; Li, E.; Li, J.; Chu, J.; Hu, Y.; Wu, D.; Jiang, L. High Performance Bubble Manipulation on Ferrofluid-Infused Laser-Ablated Microstructured Surfaces. *Nano Lett.* **2020**, *20* (7), 5513−5521.
(13) Xin, C.; Yang, L.; Li, J.; Hu, Y.; Qian, D.; Fan, S.; Hu, K.; Cai, Z.; Wu, H.; Wang, D.; Wu, D.; Chu, J. Conical Hollow Microhelices with Superior Swimming Capabilities for Targeted Cargo Delivery. *Adv. Mater.* **2019**, *31* (25), e1808226.
(14) Sitti, M.; Wiersma, D. S. Pros and Cons: Magnetic versus Optical Microrobots. *Adv. Mater.* **2020**, *32* (20), e1906766.
(15) Gladman, A. S.; Matsumoto, E. A.; Nuzzo, R. G.; Mahadevan, L.; Lewis, J. A. Biomimetic 4D printing. *Nat. Mater.* **2016**, *15* (4), 413−418.
(16) Mano, J. F. Stimuli-responsive polymeric systems for biomedical applications. *Adv. Eng. Mater.* **2008**, *10* (6), 515−527.
(17) Kim, Y.; Yuk, H.; Zhao, R.; Chester, S. A.; Zhao, X. Printing ferromagnetic domains for untethered fast-transforming soft materials. *Nature* **2018**, *558* (7709), 274−279.
(18) Liu, J.; Erol, O.; Pantula, A.; Liu, W.; Jiang, Z.; Kobayashi, K.; Chatterjee, D.; Hibino, N.; Romer, L. H.; Kang, S. H.; Nguyen, T. D.; Gracias, D. H. Dual-Gel 4D Printing of Bioinspired Tubes. *ACS Appl. Mater. Interfaces* **2019**, *11* (8), 8492−8498.
(19) Vannozzi, L.; Yasa, I. C.; Ceylan, H.; Menciassi, A.; Ricotti, L.; Sitti, M. Self-Folded Hydrogel Tubes for Implantable Muscular Tissue Scaffolds. *Macromol. Biosci.* **2018**, *18* (4), e1700377.
(20) Hu, Y.; Wang, Z.; Jin, D.; Zhang, C.; Sun, R.; Li, Z.; Hu, K.; Ni, J.; Cai, Z.; Pan, D.; et al. Botanical-inspired 4D printing of hydrogel at the microscale. *Adv. Funct. Mater.* **2020**, *30* (4), 1907377.
(21) Jeong, H. Y.; Woo, B. H.; Kim, N.; Jun, Y. C. Multicolor 4D printing of shape-memory polymers for light-induced selective heating and remote actuation. *Sci. Rep.* **2020**, *10* (1), 6258.
(22) Yoshida, K.; Onoe, H. Soft Spiral-Shaped Microswimmers for Autonomous Swimming Control by Detecting Surrounding Environments. *Advanced Intelligent Systems* **2020**, *2* (9), 2000095.
(23) Huang, H. W.; Sakar, M. S.; Petruska, A. J.; Pane, S.; Nelson, B. J. Soft micromachines with programmable motility and morphology. *Nat. Commun.* **2016**, *7* (1), 12263.
(24) Jin, Q.; Yang, Y.; Jackson, J. A.; Yoon, C.; Gracias, D. H. Untethered Single Cell Grippers for Active Biopsy. *Nano Lett.* **2020**, *20* (7), 5383−5390.
(25) Alapan, Y.; Bozuyuk, U.; Erkoc, P.; Karacakol, A. C.; Sitti, M. Multifunctional surface microrollers for targeted cargo delivery in physiological blood flow. *Science Robotics* **2020**, *5* (42), eaba5726.
(26) Bozuyuk, U.; Yasa, O.; Yasa, I. C.; Ceylan, H.; Kizilel, S.; Sitti, M. Light-Triggered Drug Release from 3D-Printed Magnetic Chitosan Microswimmers. *ACS Nano* **2018**, *12* (9), 9617−9625.
(27) Kawata, S.; Sun, H. B.; Tanaka, T.; Takada, K. Finer features for functional microdevices. *Nature* **2001**, *412* (6848), 697−698.
(28) Hohmann, J. K.; Renner, M.; Waller, E. H.; von Freymann, G. Three-Dimensional μ-Printing: An Enabling Technology. *Adv. Opt. Mater.* **2015**, *3* (11), 1488−1507.
(29) Ovsianikov, A.; Muhleder, S.; Torgersen, J.; Li, Z.; Qin, X. H.; Van Vlierberghe, S.; Dubruel, P.; Holnthoner, W.; Redl, H.; Liska, R.; Stampfl, J. Laser photofabrication of cell-containing hydrogel constructs. *Langmuir* **2014**, *30* (13), 3787−3794.
(30) Ceylan, H.; Yasa, I. C.; Sitti, M. 3D Chemical Patterning of Micromaterials for Encoded Functionality. *Adv. Mater.* **2017**, *29* (9), 1605072.
(31) Hippler, M.; Lemma, E. D.; Bertels, S.; Blasco, E.; Barner-Kowollik, C.; Wegener, M.; Bastmeyer, M. 3D Scaffolds to Study Basic Cell Biology. *Adv. Mater.* **2019**, *31* (26), e1808110.
(32) Hippler, M.; Blasco, E.; Qu, J.; Tanaka, M.; Barner-Kowollik, C.; Wegener, M.; Bastmeyer, M. Controlling the shape of 3D microstructures by temperature and light. *Nat. Commun.* **2019**, *10* (1), 232.
(33) Jin, D. D.; Chen, Q. Y.; Huang, T. Y.; Huang, J. Y.; Zhang, L.; Duan, H. L. Four-dimensional direct laser writing of reconfigurable compound micromachines. *Mater. Today* **2020**, *32*, 19−25.
(34) Schild, H. G. Poly (N-Isopropylacrylamide) - Experiment, Theory and Application. *Prog. Polym. Sci.* **1992**, *17* (2), 163−249.
(35) Goudu, S. R.; Yasa, I. C.; Hu, X.; Ceylan, H.; Hu, W.; Sitti, M. Biodegradable Untethered Magnetic Hydrogel Milli-Grippers. *Adv. Funct. Mater.* **2020**, *30*, 2004975.
(36) Peters, C.; Costanza, V.; Pané, S.; Nelson, B. J.; Hierold, C. Superparamagnetic hydrogels for Two-Photon Polymerization and their application for the fabrication of swimming microrobots. In *2015 18th International Conference on Solid-State Sensors, Actuators and Microsystems (TRANSDUCERS)*; 21−25 June 2015; 2015 ; pp 764−767.

https://dx.doi.org/10.1021/acsami.0c18221
ACS Appl. Mater. Interfaces 2021, 13, 12759−12766